EJSIT
European Journal of Science, Innovation and Technology
ISSN: 2786-4936
www.ejsit-journal.com
Volume 5 | Number 1 | 2025

Real-Time Monitoring and Control of Crude Oil Export Pumps

Nkolika O. Nwazor, Justus N. Dike and Ezekiel O. Ashaka
Department of Electrical/Electronic Engineering,
University of Port Harcourt, Rivers State, Nigeria

ABSTRACT

This paper is on the application of Model Reference Adaptive Control (MRAC) in optimizing the performance of crude oil export pumps with the goals of improving pump performance, enhancing system reliability, and increasing energy efficiency, by dynamically adjusting operational parameters in response to real-time changes in flow rates and crude oil properties. Manual control was compared to MRAC control, with a focus on error rate and accuracy rate evaluation. The MRAC method was implemented to reduce error rates and enhance control precision. The findings revealed significant improvements in both error and accuracy rates. The efficiency of the manual control is 84.5% while the efficiency of the MRAC is 90%. These results demonstrate the effectiveness of MRAC in optimizing pump operations, enhancing reliability, and reducing energy consumption. This work recommends the integration of MRAC in crude oil export pump systems to ensure sustained performance improvements, operational efficiency, efficient management of energy resources and the reduction of operational anomalies in oil export operations.

Keywords: Crude oil pump, Model Reference Adaptive control (MRAC), Adaptive control, Pump, Efficiency, Control

INTRODUCTION

Crude oil is a valuable resource essential for the world's energy demands. In the oil and gas industry, crude oil export pumps are a critical component of the oil industry, as they facilitate the transportation of crude oil from the point of extraction to refineries, storage facilities, and ships. The oil and gas industry is one of the largest industrial sectors in the world in terms of revenue generation, and pumps are essential to the smooth operation of the industry. The industry is divided into three segments: upstream, midstream, and downstream. Upstream activities involve the exploration and production of oil and gas, midstream activities involve transportation and storage, and downstream activities involve refining and selling of the final products (Mfundo et al, 2020).

Pumps used in the oil and gas industry must withstand corrosion, high temperatures, and pressures. They are used for transporting crude oil, gas, and water, and for injecting water and chemicals into wells. The pumps used in the oil and gas industry must be carefully selected based on several factors, including the type of liquid or gas being moved, flow rate, pressure, temperature, and environmental factors.

Several types of pumps are used in the oil and gas industry. They include centrifugal pumps, positive displacement pumps, diaphragm pumps, and petrochemical pumps. Centrifugal pumps are the most common type of industrial pump used in the oil and gas industry and are particularly well-suited to handle fluids that do not contain air, fumes, or large amounts of particles (Nishad et al, 2023). Positive displacement pumps, on the other hand, use spinning or reciprocating elements to drive the liquid into a contained space, providing pressure to push the liquid to its intended location. Diaphragm pumps are used during the upstream and midstream phases of crude oil refinement to pull oil into the refinery chamber, while

petrochemical pumps work at high pressure and high flow rates within a refinery system to treat or refine compounds (Goldman & Mays, 1999).

Crude oil transfer pumps are a specific type of pump used in the midstream segment of the oil and gas industry. These pumps are designed to transfer crude oil from storage tanks to transport vessels or pipelines and are normally fitted with an explosion-proof electrical motor for operations. Gear, screw, and centrifugal pump designs are available, and the characteristics of the fluid being pumped and the specific application for the pump determine which pump technology is most suitable (Ali & Goble, 2004).

LITERATURE REVIEW

The study of Mahmood and Al-Naima (2011) contributed significantly to industrial automation by proposing an internet-based distributed control system (DCS) framework designed for remote monitoring and control of oil refinery processes. This approach enables real-time data access via web browsers and facilitates centralized monitoring of complex, multi-site operations through intranet and internet technologies. Using a case study of the North Oil Refineries of Baiji (NORB) in Iraq, they demonstrate how internet-based systems can improve operational efficiency, cost-effectiveness, and safety in the oil refining industry, making real-time data accessible from any location. Ignatius et al (2023) focused on the control and monitoring systems for crude oil export pumps. The authors explored various aspects of pump operation, including efficiency, safety, monitoring mechanisms, and control strategies to optimize the performance and reliability of crude oil transfer in export operations. Priyadarshy (2016) explored strategies to enhance operational efficiency and ensure process integrity. The authors identified critical factors influencing crude oil export pump performance. The work also developed and evaluated control and monitoring strategies to optimize pump efficiency. The work in (Mfundo et al, 2020) Proposed novel approaches or technologies for enhancing safety and reliability in crude oil export operations. Demonstrated the effectiveness of the proposed control and monitoring systems through case studies or simulations.

The implementation of an automation system, particularly focusing on Distributed Control Systems (DCS), in crude oil field industries was carried out in (Guruprakash et al, 2020). Odan et al (2015) emphasized the importance of safety and efficiency in oil production and highlighted the advancements in control and automation technology. The key aim is to maintain optimal temperature and pressure during the extraction process using hydraulic fracturing simulation. The authors propose a system design based on end-user specifications and requirements, utilizing CENTUM VP software for the Field Control Station (FCS). Recent advancements in object-oriented, client-server technologies and the proliferation of Internet connectivity have provided a robust foundation for creating a unified information architecture (Boccalatte et al, 2020). This architecture enables the development of software systems that allow seamless integration of diverse applications (Goldman and Mays, 2020). As emerging standards continue to shape automation systems within industrial enterprises, the incorporation of Internet-related technologies into traditional control systems aligns these systems with both current and future technological trends. Particularly within the industrial automation sector, embedded control systems increasingly require Internet connectivity for operations such as remote plant administration, training, and supervisory activities (Aljohani, 2023). The growing role of these technologies demonstrates the potential for future development in the realm of process control systems.

METHODOLOGY

Analysis of the Existing Pump System

This equation calculates the pressure difference (ΔP) between the inlet (P_{in}) and outlet (P_{out}) of the pipeline. A significant pressure drop indicates high resistance or friction in the system, which affects flow rate and operational efficiency.

$$P_{in} = P_{out} - \Delta P \quad (1)$$

P_{in}: Inlet pressure of the pipeline.
P_{out}: Outlet pressure of the pipeline.
ΔP: Pressure drop across the pipeline.

The flow rate (Q) of crude oil through the pipeline is proportional to the square root of the pressure drop (ΔP). This equation highlights how the system's resistance, measured through pressure drop, impacts the fluid flow within the pipeline.

$$Q = K \,.\sqrt{\Delta P} \quad (2)$$

Q: Flow rate of crude oil through the pipeline.
K: Flow coefficient that accounts for the pipeline's geometry and properties.
ΔP: Pressure drop across the pipeline. Figure 1 shows the Simulink diagram of the existing pump system without the MRAC.

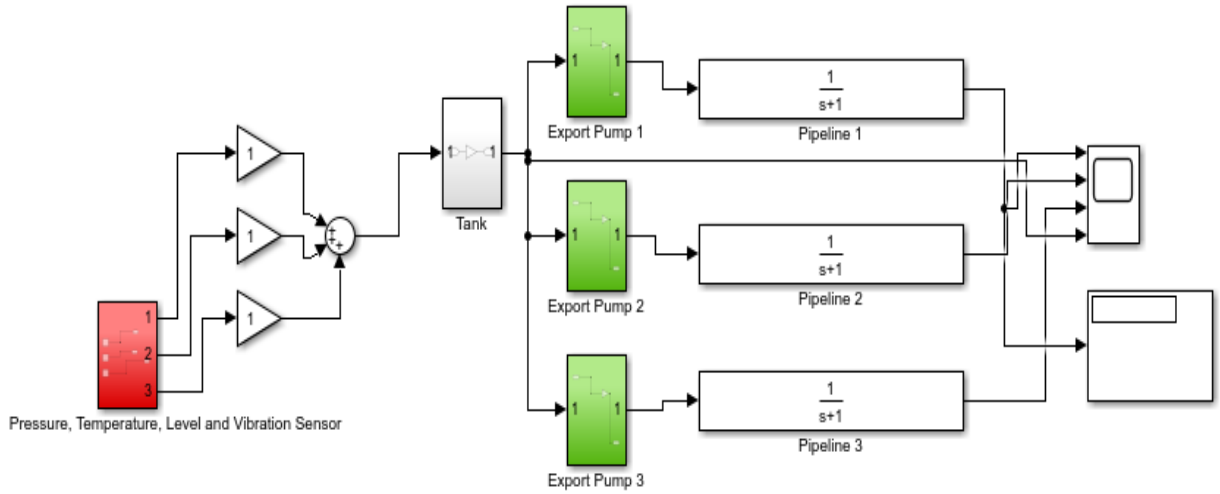

Figure 1: Existing Pump System Without MRAC Controller

This equation calculates the hydraulic power ($P_{hydraulic}$) produced by the pump. It depends on the fluid's density (ρ) gravitational acceleration (g), flow rate (Q), and the height of the pump's head (H), representing the energy transferred by the fluid.

$$P_{hydraulic} = pgQH \quad (3)$$

$P_{hydraulic}$: Hydraulic power generated by the pump.
ρ: Density of the fluid.
g: Gravitational acceleration.
Q: Flow rate.
H: Height ($head$) of the pump.
Pump efficiency (ɳ) is the ratio of the hydraulic power ($P_{hydraulic}$) output to the input electrical power (P_{input}) required to drive the pump. High efficiency indicates effective energy conversion from electrical to mechanical form.

$$ɳ = \frac{P_{hydraulic}}{P_{input}} \quad (4)$$

ɳ: Efficiency of the pump.
$P_{hydraulic}$: Hydraulic power output.
P_{input}: Electrical input power.

This equation quantifies energy loss due to friction in the pipeline. The loss is directly proportional to the square of the flow velocity (v), the pipeline length (L), and inversely proportional to the diameter (D) and friction factor (f).

$$hf = f \cdot \frac{L}{D} \cdot \frac{v^2}{2g} \tag{5}$$

hf : Frictional energy loss in the pipeline.
f: Friction factor.
L: Length of the pipeline.
D: Diameter of the pipeline.
v: Flow velocity.
g: Gravitational acceleration.

Analysis and Enhancement of System Reliability

The vibration amplitude (A_v) is the magnitude of the maximum displacement in both the $x-axis$ (x_{max}) and $y-axis$ (y_{max}) directions. It is essential for monitoring mechanical vibrations, indicating potential mechanical issues in the pump or pipeline.

$$A_v = \sqrt{x_{max}^2 + y_{max}^2} \tag{6}$$

A_v: Vibration amplitude.
x_{max}: Maximum displacement along the $x-axis$.
y_{max}: Maximum displacement along the $y-axis$.

The vibration frequency (f_v) is determined by the angular velocity (ω) of the vibrating system. It helps identify the frequency at which the system oscillates, critical for diagnosing resonance conditions that could cause mechanical failure.

$$f_v = \frac{\omega}{2\pi} \tag{7}$$

f_v: Frequency of vibration.
ω: Angular velocity of the vibrating system.

Fatigue life (N_f) quantifies how long a pipeline material can withstand stress before failure. It is inversely related to the maximum stress (S_{max}) and the material's sensitivity to stress (m).

$$N_f = \frac{C}{(S_{max})^m} \tag{8}$$

N_f: Fatigue life of the pipeline material.
S_{max}: Maximum stress experienced by the pipeline.
m: Material stress sensitivity exponent.
C: Material constant.

The stress-intensity factor (K_I) indicates the severity of stress at the tip of a crack. It is a critical parameter for assessing the potential for crack propagation and subsequent failure of the pipeline under pressure.

$$K_I = Y\sigma\sqrt{\pi a} \tag{9}$$

K_I: Stress-intensity factor.
Y: Geometry factor.
σ: Stress in the pipeline.
a: Crack length.

This equation calculates the displacement (Δx) of a pipeline subjected to an external force (F). It is influenced by the length (L), cross-sectional area (A), and material elasticity (E).

$$\Delta x = \frac{FL}{AE} \quad (10)$$

Δx: Displacement of the pipeline.
F: Applied external force.
L: Length of the pipeline.
A: Cross-sectional area of the pipeline.
E: Modulus of elasticity of the material.

Implementation of MRAC Adaptive Control System

The key idea in MRAC is to design a control law that adjusts parameters in real time to ensure the system behaves like a predefined reference model. The governing equations involve:

$$\dot{x}_m(t) = A_m x_m(t) + B_m r(t) \quad (11)$$

$\dot{x}_m(t)$: Reference model state vector (desired pump dynamics).
$A_m x_m(t) + B_m$: Reference model parameters (known, stable dynamics).
r(t): Input signal or desired setpoint (e.g., desired flow rate or pressure).

Plant Dynamics (Pump Model):

$$\dot{x}(t) = Ax(t) + Bu(t) + d(t) \quad (12)$$

x(t): Actual pump state vector.
A,B: Pump system parameters (may be unknown or time-varying). Figure 2 shows the crude oil pump control system using the MRAC controller.

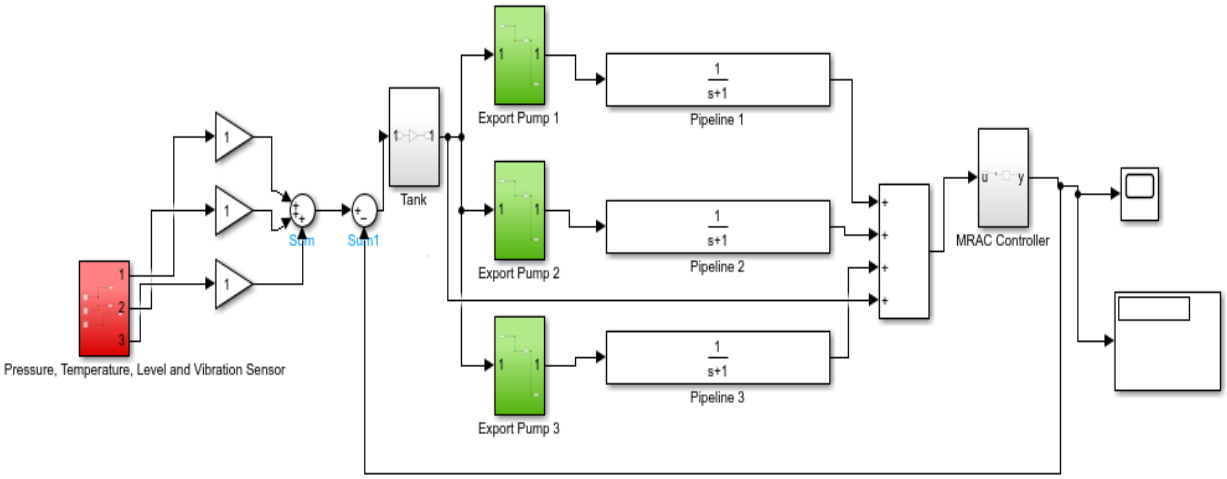

Figure 2: The Export Pump System with MRAC Adaptive Controller

Table 1, Table 2, Table 3 and Table 4 show the data used for the design and simulations.

Table 1: Export Pump 1 Shutdown and Operating Values

S/N	Export Pump EP1 Gauges	Shutdown Values	Operating Values
1	Pump oil temperature gauge	$^{70}{}^{0}$F	$^{44}{}^{0}$F
2	Pump high discharge pressure gauge	40 bar	20bar
3	Pump low suction pressure gauge	2bar	15bar
4	Low oil level gauge	50%	100%
5	High Pump vibration gauge	30 m/s^2	20 m/s^2
6	Low Water level gauge	50%	70%
7	Tank level gauge	80%	65%

Table 2: Export Pump 2 Shutdown and Operating Values

S/N	Export Pump EP1 Gauges	Shutdown Values	Operating Values
1	Pump oil temperature gauge	70 ^{0}F	40 ^{0}F
2	Pump high discharge pressure gauge	40 bar	30bar
3	Pump low suction pressure gauge	2bar	15bar
4	Low oil level gauge	50%	100%
5	High Pump vibration gauge	30 m/s^2	15 m/s^2
6	Low Water level gauge	50%	100%
7	Tank level gauge	80%	70%

Table 3: Export Pump 3 Shutdown and Operating Values

S/N	Export Pump EP1 Gauges	Shutdown Values	Operating Values
1	Pump oil temperature gauge	$^{70\ 0}$F	$^{44\ 0}$F
2	Pump high discharge pressure gauge	40 bar	35 bar
3	Pump low suction pressure gauge	2bar	15bar
4	Low oil level gauge	50%	100%
5	High Pump vibration gauge	30 m/s^2	20 m/s^2
6	Low Water level gauge	50%	70%
7	Tank level gauge	80%	74%

Table 4: Daily Data

Time (Day)	Pressure (Bar)	Temperature (°C)	Vibration (m/s²)	Level Gauge (%)	Category
Day 1	50	300	1	46.30%	Safe
Day 2	52	299.5	1.05	48.15%	Safe
Day 3	54	299	1.1	50.00%	Safe
Day 4	56	298.5	1.15	51.85%	Safe
Day 5	58	298	1.2	53.70%	Safe
Day 6	60	297.5	1.25	55.56%	Safe
Day 7	62	297	1.3	57.41%	Safe
Day 8	64	296.5	1.35	59.26%	Safe
Day 9	66	296	1.4	61.11%	Safe
Day 10	68	295.5	1.45	62.96%	Safe
Day 11	70	295	1.5	64.81%	Safe
Day 12	72	294.5	1.55	66.67%	Moderate
Day 13	74	294	1.6	68.52%	Moderate
Day 14	76	293.5	1.65	70.37%	Moderate
Day 15	78	293	1.7	72.22%	Moderate
Day 16	80	292.5	1.75	74.07%	Moderate
Day 17	82	292	1.8	75.93%	Critical
Day 18	84	291.5	1.85	77.78%	Critical
Day 19	86	291	1.9	79.63%	Critical
Day 20	88	290.5	1.95	81.48%	Warning
Day 21	90	290	2	83.33%	Warning
Day 22	92	289.5	2.05	85.19%	Warning
Day 23	94	289	2.1	87.04%	Warning
Day 24	96	288.5	2.15	88.89%	Warning
Day 25	98	288	2.2	90.74%	Emergency
Day 26	100	287.5	2.25	92.59%	Emergency

Evaluation of Error Rate Comparison for Both Manual and Automated Control

To compare the error rate and accuracy of manual control versus MRAC control for a system like the Soku export pumps, we can define and analyze their performance metrics. These metrics are based on the deviation of the system output from the desired output and the ability to track a setpoint over time.

Tracking Error e(t): The difference between the desired output yd(t) and the actual system output y(t):

$$e(t) = y_d(t) - y(t) \tag{13}$$

Manual Control Error ($e_{manual}(t)$): The error when the system is under manual control.
MRAC Control Error ($e_{MRAC}(t)$)**:** The error when the system is under MRAC control.

$$error\ rate = \frac{\Delta e(t)}{\Delta t} \tag{14}$$

The error rate quantifies the system's responsiveness in reducing error over time. It can be calculated as:
For manual control

$$Error\ Rate_{manual}\ \frac{e_{manual}(t) - e_{manual}(t-\Delta t)}{\Delta t} \tag{15}$$

For MRAC control

$$Error\ Rate_{MRAC}\ \frac{e_{MRAC}(t) - e_{MRAC}(t-\Delta t)}{\Delta t} \tag{16}$$

Evaluation of Accuracy Comparison for Both Manual and Automated Control

Accuracy measures the proximity of the system output to the desired value, typically represented as the complement of the normalized error.
Instantaneous Accuracy:

$$Accuracy(t) = \frac{|e(t)|}{|y_d(t)|} \tag{17}$$

RESULTS AND DISCUSSION

Improved Pump Efficiency and Enhanced Reliability (Reduced Failure Rate)

Figure 3 explains the results improved pump efficiency using MRAC. It can be shown that the pump efficiency started increasing from 0.8% to 6 % of the efficiency axis in 100 seconds. This signifies that with the MRAC being adopted to the pump system, instead of efficiency will reduce, the efficiency increases over time. This shows that the MRAC method has a very high positive impact in the pump control system by adjusting the pump effectively.

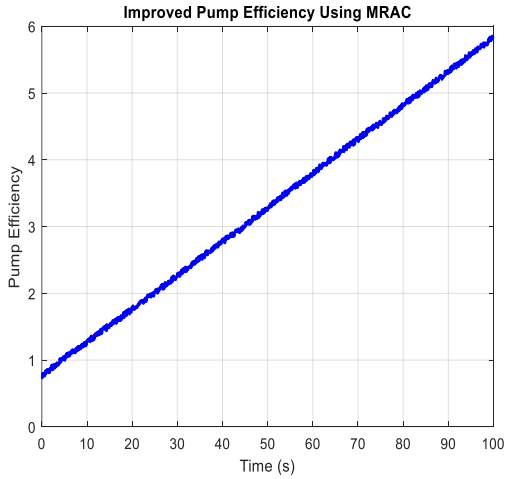

Figure 3: Improved pump Efficiency Using MRAC

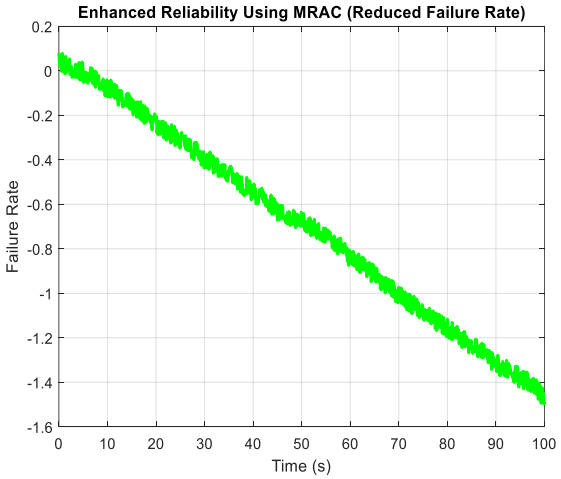

Figure 4: Enhanced Reliability using MRAC

The impact of MRAC controller is shown in Figure 4. The impact indicates that the failure rate is reducing instead of increasing over time, which is ideal for an effective system. The reduction of the failure rate is an example of an effective system. The result shows that the failure rate at 0.1 decreases gradually to -1.5 over time at 100 seconds this shows the effectiveness of the use of MRAC technique.

Increased Safety, Better Decision Making and Reduced Maintenance Cost

One of the major factors of the MRAC system to also provide a preventive measure of safety and to reduce damage. The results here have shown that with the MRAC controller, safety has been improved and incidents has been reduced over time. The results in Figure 5 shows the reduce incident over time, the safety incidents reduced from 0.2 to -70 to prove the effectiveness of the system.

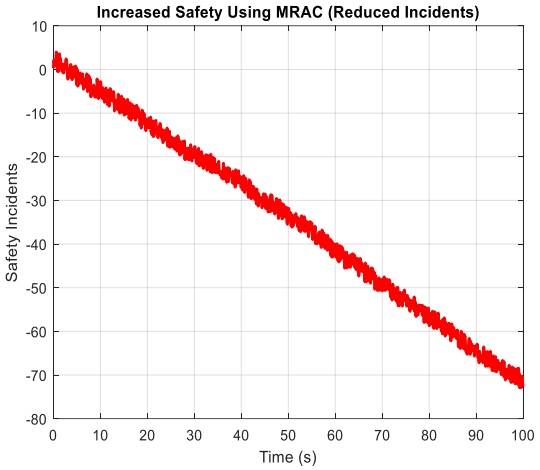

Figure 5: Increased Safety Using MRAC

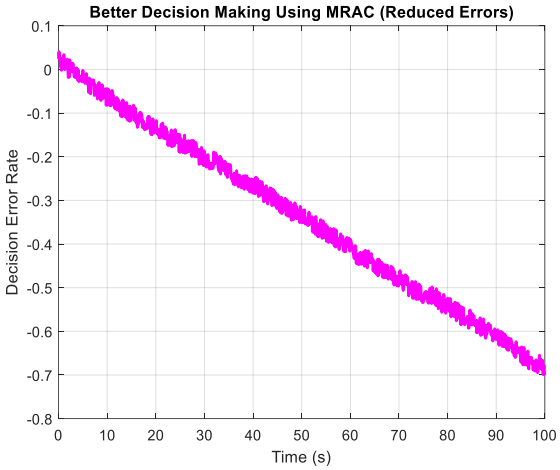

Figure 6: Better Decision Making Using MRAC

The results in Figure 6 show that the MRAC system is better at making decisions, and this made it have a very low decision error rate. The results show that over time the decision error rate is reduced overtime. The results in figure 6 show that decision error was reduced from 0.01 to -0.7 at 100 seconds.

Figure 7 shows the trends of the maintenance cost reduction over time. Due to the effectiveness of the MRAC technique, it shows that maintenance cost reduction of the pumps was reduced from 1000 currency units to -15000 currency units in 100 seconds.

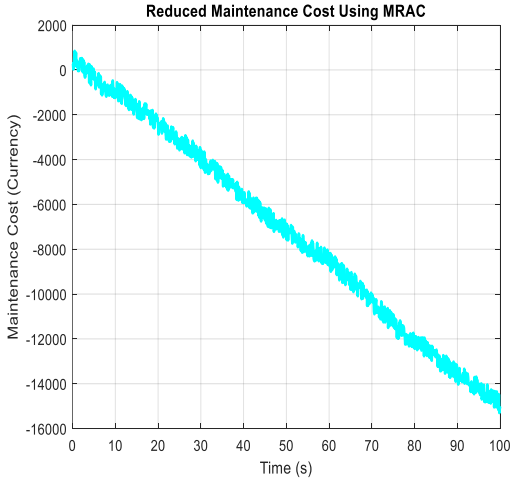

Figure 7: Reduced Maintenance Cost Using MRAC

Pump Oil Temperature and High Discharge Pressure Response

Figure 8 results show the export pump oil temperature response, for export pump 1. The result for the shutdown is 70°F, while the operating condition stabilizes at 44°F. and the same for export pump 2, and for export pump 3. The results show that the temperature remains at 70°F in the shutdown state and reduces further to 44°F. This shows that the temperature dropping down from the shutdown to operating temperature is consistent.

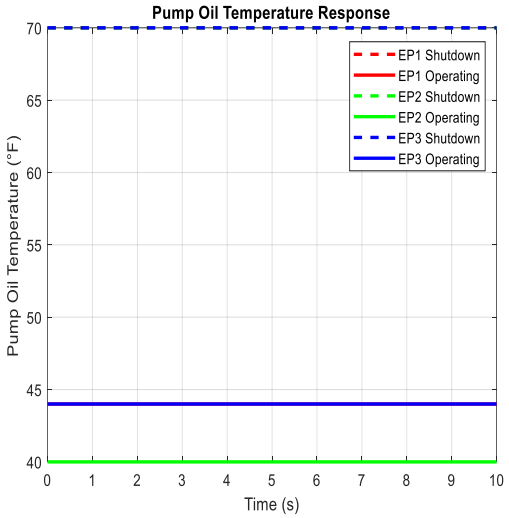

Figure 8: Pump Oil Temperature Response

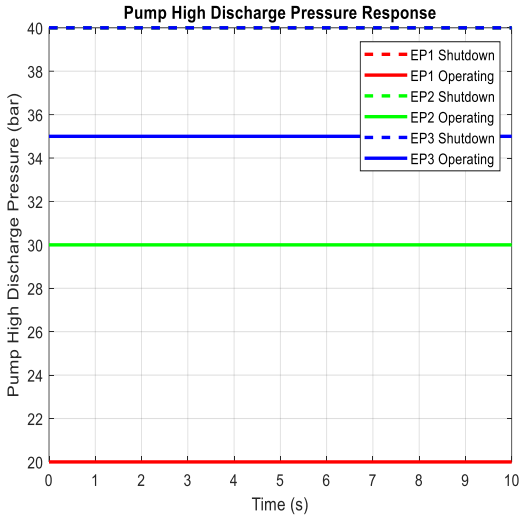

Figure 9: Pump High Discharge Pressure Response

The very high discharge rate of the pressure response of the 3 export pumps is shown in Figure 9. It shows that for EP1 discharge pressure is 40 bar and dropped down to 20 bar during operation, for EP2 the shutdown discharge pressure is 40 bar in and 30 bar during the operation period and EP3 decreases from 40 bar to 35 bar during operation.

Pump Low Suction Pressure and Low Oil Level Response

Figure 10 shows the pump's low suction pressure response. The results show that EP1 has a 2-bar pressure suction rate during shutdown and increased to 15 bar during operation. EP2 and EP3 have the same behavior, 2 bar suction pressure rate for shutdown and increased to 15 bar suction pressure rates at operation.

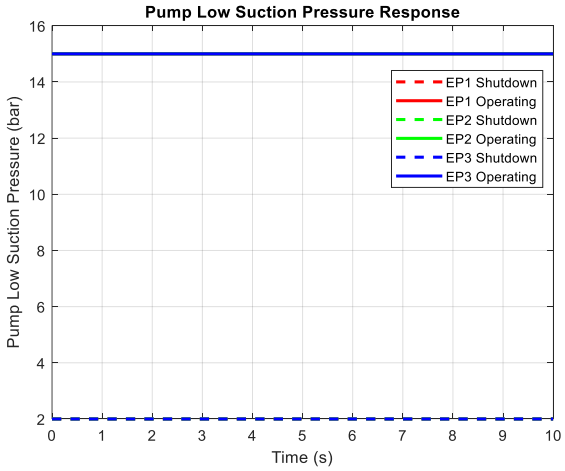

Figure 10: Pump Power Low Suction Pressure Response

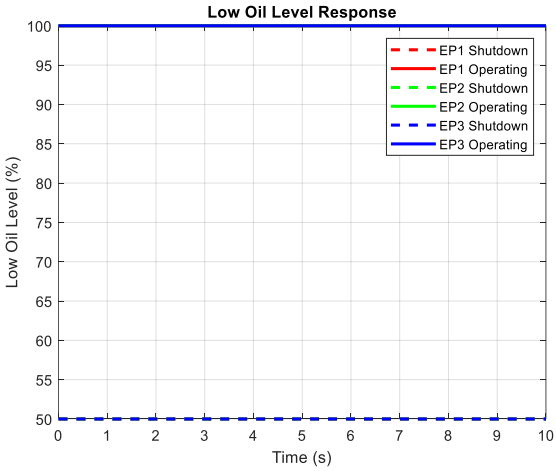

Figure 11: Low Oil Level Response

The results in Figure 11 show the low oil level for EP1, EP2 and EP3 shut down at 50%, and increases to 100% during operation for EP1, EP2 and EP3. The oil at 50% shows the consumption of the oil or redistribution.

High Pump Vibration Response and Low Water Level Response

Figure 12 results show the vibration levels in each of the export pumps. During shutdown, the three pumps' vibration level is at 30 m/s². During the operation of the export pumps, the vibrations change over time, for EP1 the vibration level increases to 20 m/s², EP2's vibration level increases from 15 to 30 m/s², and EP3's vibration level rises from 20 to 30m/s². the increment of the is the export pumps is due to mechanic stress.

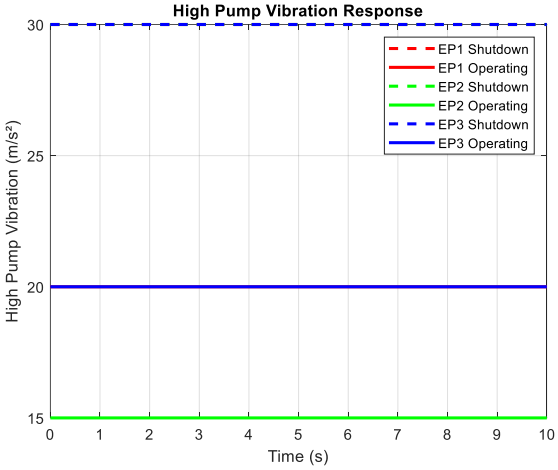

Figure 12: High Pump Vibration Response

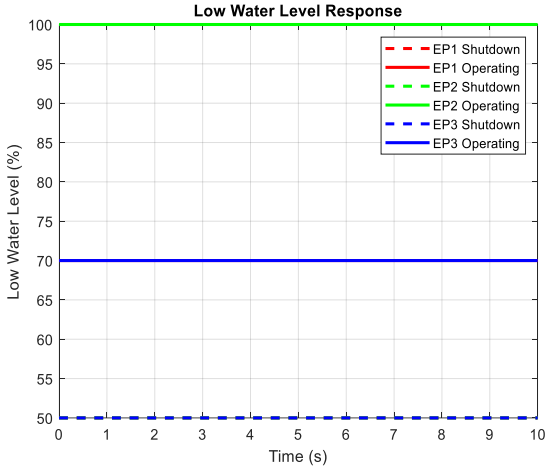

Figure 13: Low Water level Response

The results in Figure 13 depicts the response of the low water for the three export pumps. During shutdown period the export pumps, the water levels go below 50%. While during operation, the water level increase from 50% to 100% for EP1, EP2 and EP3.

Tank Level Response

Figure 14 shows the tank level for each pump. Each pump has an 80% level at shutdown, and the levels decrease further during operation to 65% for EP1, 70% for EP2 and 74% for EP3. The reduction in the pump size shows the difference in pump capacity and size.

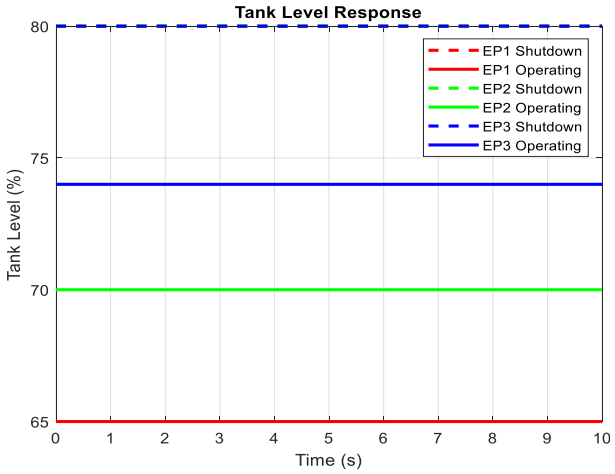

Figure 14: Tank Level Response

Pump Oil Temperature and Discharge Pressure

The results in the first subplot of Figure 15 compare the oil temperature level pumps under manual control and MRAC conditions. The results show that the red fluctuates around 70°F and reduced to 65°F. The blue curve shows the MRAC control and how effective it is over the manual control. The MRAC control starts at a temperature of 60°F and stabilizes at 68°F faster than the manual control in 10 seconds. The second subplot of Figure 15 shows the pressure discharge performance under manual and MRAC control. Under conventional control, the red swings significantly within 40 bars to 30bars. This shows the inefficiencies of the conventional method. However, the MRAC pressure controller is represented by the blue curve, which starts with a very sharp adjustment and quickly stabilizes at a pressure of 38 bar within 10 seconds. The reduction in overshoot illustrates the precision of the MRAC.

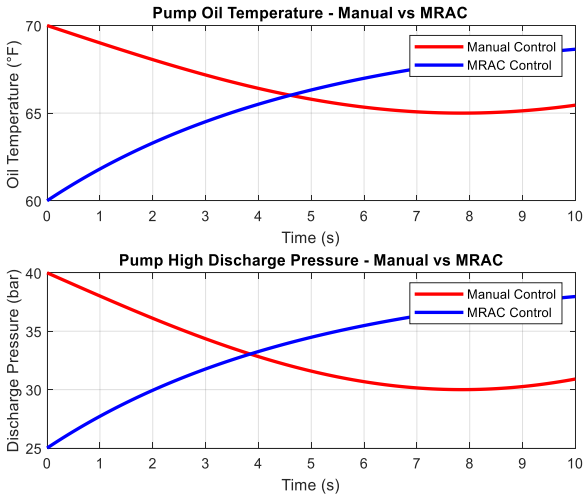

Figure 15: Pump Pressure Discharge

Pump Efficiency Comparison

The efficiency comparison of the pump is shown in figure 16 between the manual control and the MRAC control over time, the results shows that the red line represent the manual control, which the has over 80% to 84.5% in 10 seconds efficiency indicating it inefficiencies to maintain precision. The blue line shows the efficiency of the MRAC system starting from 88% and stabilizing at 90% in 10 seconds almost 5.5% higher than the manual control.

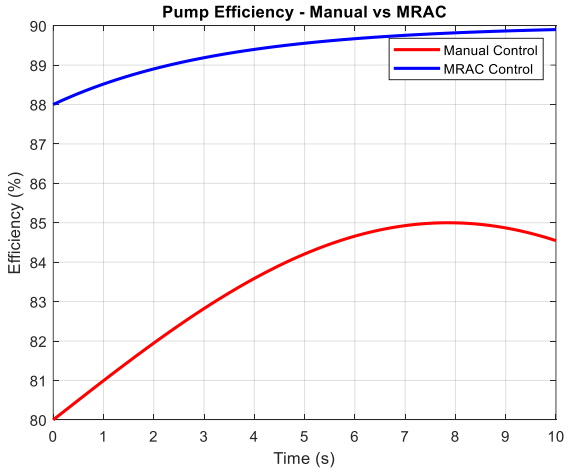

Figure 16: Pump Efficiency Comparison

CONCLUSIONS

This study evaluated the performance of the three crude oil export pumps. The study also simulated the performance of the MRAC when controlling the three pumps using MATLAB/SIMULINK. Evaluation of the performance of the MRAC control system in the crude oil pump control was investigated, afterwards the performance of the system was compared to the conventional manual control system over time. The study showed that the MRAC system significantly improves the performance of the pumps, optimized the efficiency of the pumps, improve the reliability of the pump, and the safety of the pump overtime. The study shows that figure 3 has an improved pump efficiency from 0.8% to 6 %, while the failure rate of the system reduced from 0.2 to -1.5 in figure 4. Safety incidents were also reduced from 0.02 to -70 overtime as shown in figure 5. Decision errors was also reduced from 0.01 to -0.7 when MRAC was applied in figure 6 and figure 7 shows that overtime the maintenance cost of the pump reduced from 1000 to -15000 units. The study also evaluated the MRAC stabilized oil temperatures and discharge pressures in figure 8 and 9. The study also evaluated the management of suction pressure and the levels of the oil effectively as shown in figure 10 and 11. The comparison of both performance of MRAC pump control and the conventional pump control was carried out, and it was shown in the figure 16 that the manual pump control has an efficiency that increased from 80 and stabilized at 84.5% efficiency while the MRAC efficiency increased from 88% to 90% in 10 seconds. This shows that the MRAC system has a better performance than the conventional controller.

REFERENCES

Alabi, O. A., Olukunle, O. F., Ojo, O. F., Oke, J. B., & Adebo, T. C. (2022). Comparative study of the reproductive toxicity and modulation of enzyme activities by crude oil-contaminated soil before and after bioremediation. *Chemosphere, 299*. https://doi.org/10.1016/j.chemosphere.2022.134352

Ali, R., & Goble, W. (2004). Optimal near real-time control of water distribution system operations, *The Instrumentation, Systems, and Automation Society, 22*(40), 15-27.

Boccalatte, A., & Coccoli, M. (2020). Future directions of internet-based control systems. *Journal of Computing and Information Technology, 10*(2), 21-30.

Goldman, F. E., & Mays, L. W. (1999). The application of simulated annealing to the optimal operation of water systems. In *Proceedings of the WRPMD'99 Preparing for the 21st Century,* Tempe, AZ, USA, June 6–9.

Guruprakash, S., Rajendra, S., & Singh, P. (2020). Automation and supply of distributed control systems for crude oil field industries. *International Research Journal of Engineering and Technology, 7*(6), 6155. https://www.irjet.net

Ignatius, G. I., Nawawi, M. G. M., Mohd, Z. J., & Farah, B. S. (2023). Environmental effects from petroleum product transportation spillage in Nigeria: A critical review. *Environmental Science and Pollution Research, 31*(4), 1–29. https://doi.org/10.1007/s11356-023-31117-z

Mahmood, M., & Al-Naima, F. (2011). An internet-based distributed control systems: A case study of oil refineries. *Energy and Power Engineering 3*(3), 25-37. https://www.researchgate.net/publication/236018681

Mahmoud, A. A. B., & Piratla, K. R. (2019). Optimal operational control of water pipeline systems using real-time scheduling framework. In *Pipelines 2019: Planning and Design*, 15(3) 243-248.

Mfundo, N., Kapil, G., & Madindwa, M. (2020). Causes and impact of human error in maintenance of mechanical systems. *MATEC Web of Conferences, 05001*. https://www.matec-conferences.org/articles/matecconf/pdf/2020/08/matecconf_eppm2018_05001.pdf

Muqeet, M. A., Najeeb, M. A., Akbar, F., & Ali, S. (2015). PLC and SCADA-based control of continuous stirred tank reactor (CSTR). *International Journal of Innovative Research in Electrical, Electronics, Instrumentation and Control Engineering*, *3*(12), 45-54.

Nishad, A. D., Yadav, A. K., & Dwivedi, A. (2023). PLC & SCADA-based automation in boiler systems enhancing energy efficiency: A review. *International Journal*, *10*(1), 13-22.

Odan, F. K., Reis, L. F. R., & Kapelan, Z. (2015). Real-time multiobjective optimization of operation of water supply systems. *Journal of Water Resources Planning and Management*, *141*(1), 40-51.

Priyadarshy, S. (2016). IoT revolution in oil and gas industry. In H. Geng (Ed.), *Internet of Things and Data Analytics Handbook* (Ch. 31, pp. 513–520). Wiley. https://doi.org/10.1002/9781119173601.ch31

Aljohani, A. (2023). Risk mitigation and agility: Predictive analytics and machine learning for real-time supply chain. *Sustainability*, *15*(20), 15088. https://doi.org/10.3390/su152015088